NANO LETTERS

2007
Vol. 7, No. 8
2220−2226

Production and Characterization of Coaxial Nanotube Junctions and Networks of CN_x/CNT

X. Lepró, Y. Vega-Cantú, and F.J. Rodríguez-Macías

Advanced Materials Department, IPICYT, Camino a la Presa San José 2055, Col. Lomas 4a sección, San Luis Potosí, 78216, México

Y. Bando and D. Golberg

Advanced Materials Laboratory and Nanomaterials Laboratory, National Institute for Materials Science, Namiki 1-1, Tsukuba, Ibaraki 305-0044, Japan

M. Terrones*

Advanced Materials Department, IPICYT, Camino a la Presa San José 2055, Col. Lomas 4a sección, San Luis Potosí, 78216, México, and International Center for Young Scientists (ICYS), National Institute for Materials Science, Namiki 1-1, Tsukuba, Ibaraki 305-0044, Japan

Received March 20, 2007; Revised Manuscript Received May 18, 2007

ABSTRACT

Novel coaxial structures consisting of nitrogen-doped carbon nanotube (MWNTs-CN_x) cores with external concentric shells of pure carbon were produced by the pyrolysis of toluene over Fe-coated MWNTs-CN_x. These materials were thoroughly characterized by SEM, HRTEM, X-ray diffraction, and TGA; a possible growth scenario for their formation is also proposed. In addition, these coaxial structures were able to form 2D and 3D covalent networks that mainly exhibited T-, Y-, and on-type morphologies. The two-step technique presented here could be further developed to fully control the growth of these new coaxial structures, study of individual junctions, and it could be used to create periodic nanotube networks, in which the heterocable structure could find applications in nanoelectronics.

Single-walled carbon nanotubes (SWCNTs) appeared to be observed for the first time by Oberlin and Endo[1] in 1976, but only after the structural identification of multiwalled carbon nanotubes (MWCNTs)[2] in 1991 and SWCNTs in 1993,[3,4] nanotubes started to be extensively studied from both theoretical and experimental standpoints. The molecular structure of pure carbon nanotubes (CNTs) consists of rolled graphene sheets (sp^2 hybridized carbon) with outstanding mechanical properties (Young's modulus in the TPa range[5]) because the C−C bond in graphene is one of the strongest in nature. In addition, the angle at which the hexagonal pattern arranges with respect to the main tube axis provides a metallic or semiconductor nature to the CNTs.[6,7] Because of those properties, CNTs could be considered as important blocks for building novel reinforced materials[8] and nanoscale electronic devices.[9−12] In particular, 2D and 3D nanotube networks consisting of covalently bonded nanotubes could be used as composite fillers,[6] catalyst supports for fuel cells,[13,14] filters,[15] nanoelectronic circuits,[16,17] and for other applications.[13,18,19] Therefore, a facile and low-cost synthetic route to create 2D and 3D nanotube junctions (using SWCNTs or MWCNTs) is inevitably required, as several authors have pointed out.[18−20]

Unfortunately, it has been difficult to interconnect covalently pure carbon nanotubes due to the chemical inertness (similar to graphite) of their surface. Some authors have succeeded in covalently welding SWCNTs by introducing defects (e.g. vacancies, interstitial atoms, edges, etc.) on the tubes' surface using electron irradiation processes.[21,22] However, such a technique is not completely controllable, and it does not allow large-scale production of multiterminal junctions.

An alternative route to interconnect nanotubes consists in using doped-carbon nanotubes (which are more chemically reactive than pure carbon nanotubes). Doping results in the formation of active sites on the tube surfaces without the need for harsh oxidation treatments. It also allows one to modify the electronic properties of the tubes by replacing carbon atoms with atoms containing additional electrons (donors) or fewer valence electrons (acceptors), similar to the techniques used in the semiconductor industry.[23] Particularly, nitrogen in doped carbon nanotubes (CN_x) acts as electron donor. Thus CN_x exhibit an increased number of electronic states close to the Fermi level and could be metallic depending on the amount of N in the tubular systems.[24] For these reasons, the fabrication of covalent CN_x nanotube junctions could be an important development in nanotube

* Corresponding author. E-mail: mterrones@ipicyt.edu.mx.

10.1021/nl0706502 CCC: $37.00
Published on Web 07/21/2007

technology. The increased reactivity due to the nitrogen sites also facilitates the attachment of substances such as gold nanoparticles[25] and biomolecules.[26] However, such modifications have still relied on an oxidation treatment as a first step.

In this letter, we demonstrate that the deposition of Fe nanoparticles on carbon nanotubes is facilitated by the presence of nitrogen sites on the CN_x nanotube surface and that these nanoparticles act as catalysts for the subsequent growth of CNTs, thus creating fascinating junctions and networks. These junctions consist of concentric heteronanocables with MWNT-CN_x cores and pure carbon cylinders on the outside (CN_x@CNT). These structures could then display an inner tubular structure of higher conductivity (due to the nitrogen doping) and a less-conductive sheath. To the best of our knowledge, these novel structures have not previously been synthesized or even proposed theoretically.

Multiwalled nitrogen-doped carbon nanotubes (MWNT-CN_x) were synthesized via chemical vapor deposition (CVD).[7,27,28] In brief, we sprayed a solution of ferrocene ($FeCp_2$; Aldrich, reagent grade; 5 wt %) in benzylamine (C_7H_9N; Aldrich, reagent grade), under Ar flow, into a quartz tube placed inside a two-stage furnace operating at 800 °C. The nanotubes were collected from the inner walls of the quartz tubes.

We deposited Fe nanoparticles on the as-produced MWNTs-CN_x using two different approaches. The first involved the use of complex iron salts: here, 10 mg of MWNT-CN_x were dispersed in 10 mL of an aqueous solution of CH_3COOH (75% v/v) by ultrasonication for 20 min (Cole-Parmer model 8891, 42 kHz). Subsequently, 63.4 mg of potassium hexacyanoferrate(III), $K_3[Fe(CN)_6]$, (Aldrich, reagent grade), were added to the system, corresponding to an Fe/C atomic ratio of 0.23. This mixture was later placed in an ultrasonic bath for 1 h at room temperature to ensure a homogeneous dispersion. Finally, the suspension was heated under an Ar flow at ca. 100 °C with reflux but allowing slow evaporation of the solvents.

The second approach for anchoring Fe clusters on MWNT-CN_x consisted in mixing MWNT-CN_x with dimethylformamide (DMF) (Sigma-Aldrich, reagent grade) in concentrations of around 1 mg/mL. The nanotubes were subsequently dispersed by ultrasonication for 1 h, then an acidic Fe^{+3} aqueous solution (10.3 mM; from an $FeCl_3$ solution, pH adjusted to 3 using CH_3COOH) was added dropwise to the nanotube dispersion. This system was then dried in a hot plate at ca. 80 °C under continuous stirring.

After the Fe was deposited on MWNT-CN_x, we introduced the products (obtained using both methods described above) back into a CVD system.[28,29] The metal-coated nanotubes were placed inside alumina boats in the middle part of the quartz tube corresponding to the second furnace (see above). Argon was flowed over the sample (0.3−0.5 L/min), and once the furnace temperature reached 825 °C, pure toluene (C_7H_8; Fermont), *without any ferrocene catalyst*, was sprayed inside the tube for 5 min.

The final products were analyzed by several methods: (1) SEM (FEI-Philips SFEG-XL30) operating at 10−15 keV and equipped with an EDAX detector for elemental microanalysis by energy dispersive X-ray analysis (EDX). (2) HRTEM (field emission JEOL-JEM-3000F) with a 300 keV acceleration voltage and equipped with a Gatan 766 2D-DigiPEELS detector. (3) XRD (Brucker D8) equipped with a Cu anode ($\lambda = 1.5406$ Å) operated at 35 kV, 25 mA, and 293 K from 10° to 110° in 2θ angle. (4) TGA (Thermo Haake, Cahn VersaTherm HS) heating at 5 °C/min to 800 °C in air.

SEM images of the products obtained after the second CVD treatment of the Fe-coated MWNT-CN_x are shown in Figure 1. The results were similar for the two Fe deposition methods: the metal particles catalyze the growth of new nanotubes on the CN_x nanotube surface, producing randomly interconnected nanotube networks (Figure 1a−c) with different kinds of junctions. Among those, we note the following general types: (1) Y-junctions (Figure 1d,e), (2) T-type junctions (Figure 1f), (3) multibranched junctions (Figure 1g,h), and "on-junctions" (Figure 1i). It is also important to note that the diameter of the coaxial nanotubes increased from ca. 35 nm (measured for the pristine MWNTs-CN_x, not shown here) to ca. 100 nm after the second CVD treatment as a result of the carbon layer deposited on the MWNT-CN_x. It is also noteworthy that the networked nanotube material appears to be more compact than the pristine CN_x nanotube material, which has a porous texture.

We found that the highest yields of junctions are produced when using an Ar flow of 0.3 L/min and spraying the toluene solution for 15 min.

To examine the detailed structure of the junctions, we carried out HRTEM studies. Figure 2a shows a Y-junction, where the MWNT-CN_x can be identified in the central core by their bamboo-like structure. Higher magnifications of these locations (Figure 2b,c) reveal the crystalline planes of the MWNT-CN_x covered by less-crystalline graphene layers, with an interlayer spacing (calculated via Fast Fourier transform (FFT) analysis) of ca. 0.08 Å larger than that of the MWNT-CN_x cores. We named these coaxial structures CN_x@CNT. It is noteworthy that we expected new nanotube growth catalyzed by the deposited iron nanoparticles, but the formation of nested carbon cylinders around the MWNT-CN_x was a surprising result.

An "on-junction", shown in Figure 2d, also displays an internal core of MWNT-CN_x surrounded by carbon layers. The "graphitic" planes of a T-junction like the one shown in Figure 2f can be observed in a high-magnification TEM micrograph in Figure 2e. Here we again identify two distinct types of graphene sheets (the inner MWNT-CN_x and the outer carbon layers). We also note that the normal grown tube (pure carbon) has a diameter half that of the main nanotube stem and it has lower crystallinity than that of MWNT-CN_x. From Figure 2e, it is also clear that the tube has grown from the surface of the CN_x tubes and, even if there is no sign of a complete merge between the tubes, the graphitic planes at the junction appear well adhered, thus the junction is expected to be mechanically stable.

We believe that additional thermal annealing of these junction structures could increase the crystallinity of the

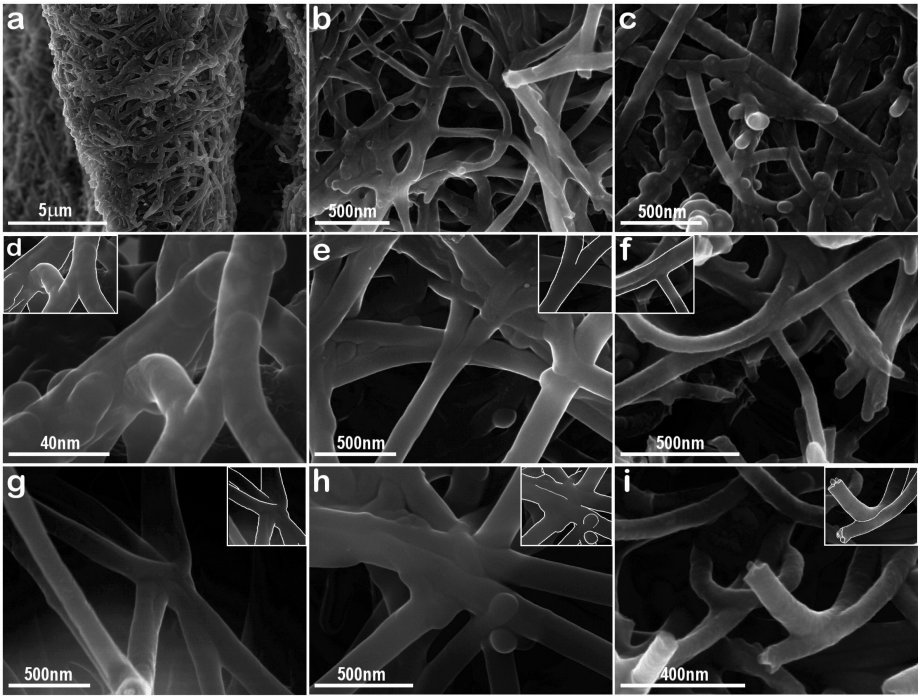

Figure 1. SEM images of nanotube junctions: (a) overall morphology of the CN_x@CNT networks; (b) and (c) higher magnification images showing different ways in which the nanotubes are joined; (d) and (e) are representative images of "Y"-junctions; (f) a "T"-junction; (g) and (h) show multibranched structures, and (i) exhibits one nanocable embedded over another, denoted as an "on-junction".

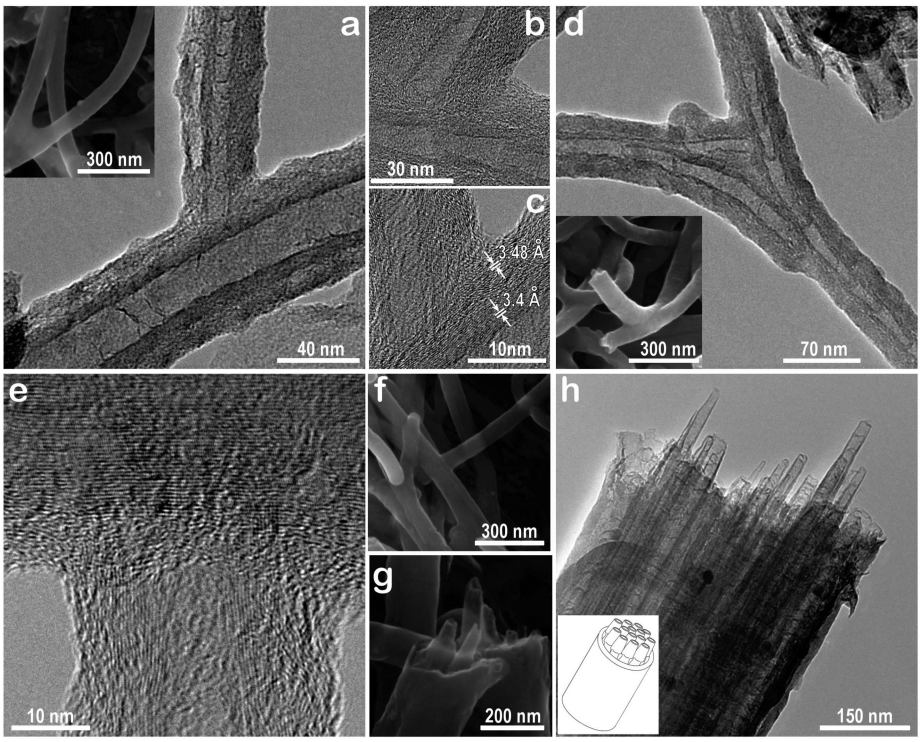

Figure 2. HRTEM images of the different heterojunction structures. (a) A typical "Y"-junction consisting of an inner core (MWNT-CN_x), and an outer shell of carbon layers. (b,c) Other examples of "Y" junctions showing higher crystallinity of the MWNT-CN_x with respect to the outer shell, which has a larger interlayer spacing (by ca. 0.08 Å). (d) An "on-junction" (the inset shows an SEM image of this kind of junction), the bamboolike structure of the MWNTs-CN_x core is clearly observed. (e) A "T"-junction showing graphene planes perpendicular to the core tube. The poorer crystallinity of the external graphene layers is easily noted and there is no sign of total fusion between tubes. (f) SEM image of a "T"-junction. (g) SEM image showing the tips of MWNTs-CN_x inside a broken heteronanocable structure, and (h) a bundle of MWNTs-CN_x inside MWCNTs (CN_x@CNT). A schematic representation of the structure of these cables can be seen in the inset.

carbon layers wrapping the MWNTs-CN_x, thus resulting in an increase of the mechanical strength of these structures.

Among the products, by SEM and TEM, we also observed bundles of MWNTs-CN_x covered by carbon layers, thus

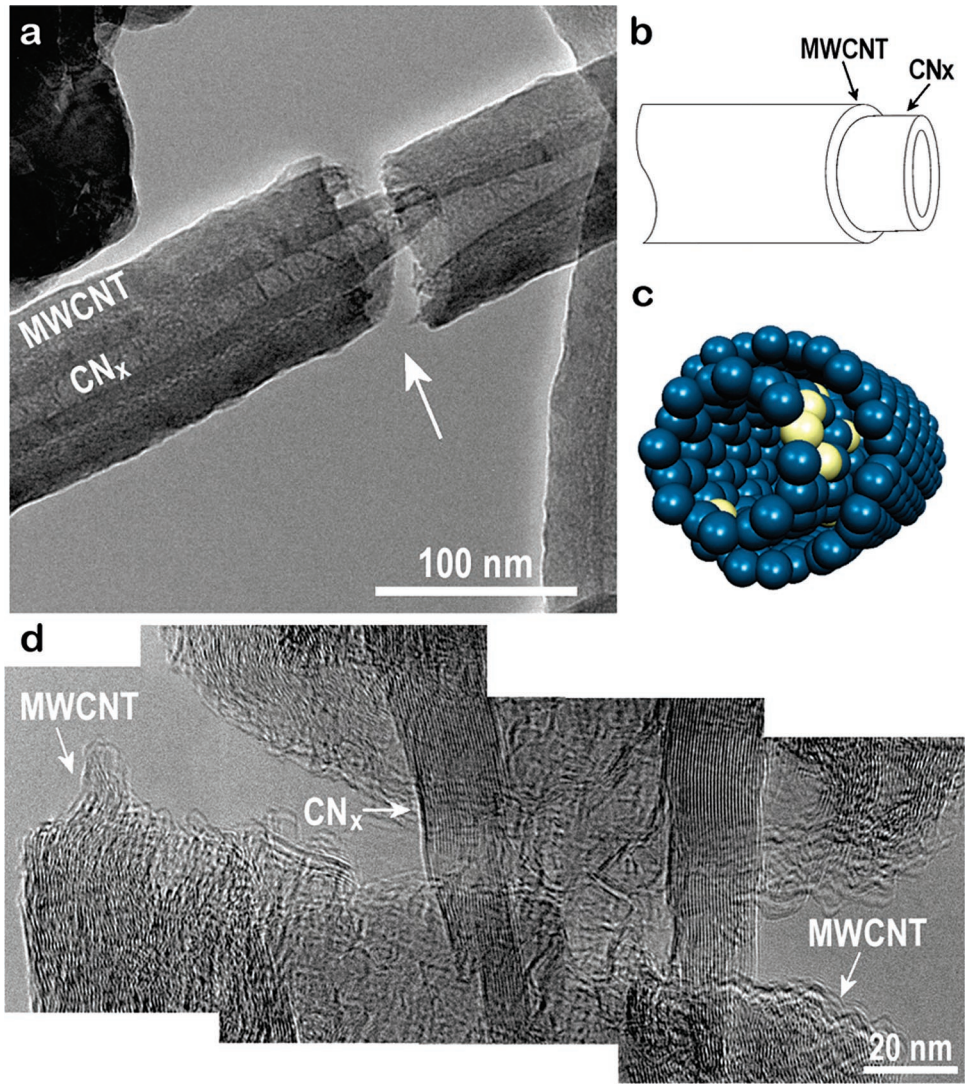

Figure 3. Images and structure of coaxial heteronanotubes. (a) A HRTEM image of a broken coaxial tube CN_x@CNT showing different kinds of fractures for the inner and the outer shells. (b) Schematic representation of the coaxial heteronanotubes. (c) Molecular model representing a CN_x inside a CNT (only a layer of each type of carbon nanotube is shown for clarity), bright atoms are N, darker ones are C, and (d) HRTEM image of the broken part of the coaxial cable marked with an arrow in (a).

forming a different type of heteronanocables (see Figure 2h and schematic diagram). These multitubular arrays might consist of metallic MWNT-CN_x tubes coated by a more-defective (less conductive) carbon nanotube. To the best of our knowledge, this kind of random networks and heteronanocables, where the core is a doped nanotube, have not been reported hitherto; even if different types of junctions have been reported, they only consist of pure carbon nanotubes, and the morphologies are different from those described in this letter.

The HRTEM image in Figure 3 clearly shows the concentric arrangement of different types of nanotubes in a broken coaxial cable, with a bamboolike MWNT-CN_x core and a pure carbon MWNT on the outside. The inner and the outer shells reveal two kinds of fractures: the MWNT-CN_x appears to break by sliding of the cup-stacked graphene layers, whereas the outer MWCNT seems to crack as a brittle material. A molecular model of the coaxial nanotube cable is represented in Figure 3c, in which the N atoms are depicted in a light color and C atoms are dark. The broken part (marked with an arrow in Figure 3a) can be seen in more detail in Figure 3d. Here, the atomic planes belonging to the MWNTs-CN_x appear to be more crystalline than those belonging to the outer MWCNTs shell.

As mentioned above, the Fe clusters deposited on the surface of MWNTs-CN_x catalyze the formation of new MWCNTs by toluene thermolysis. Figure 4a illustrates the mechanism for this phenomenon; the deposited iron nanoparticles cluster together and eventually form iron nanorods (180 nm length by 30 nm width in the example shown), which we believe act as a template for the growth of the new carbon nanotubes. This metal cluster coalescence (Figure 4b) could be due to an annealing process occurring while increasing the system temperature before the CVD treatment with pristine toluene. Other examples of the interface between the metal and the MWNT-CN_x tube surface are displayed in Figure 4b,c. EELS mapping of 4c confirms that

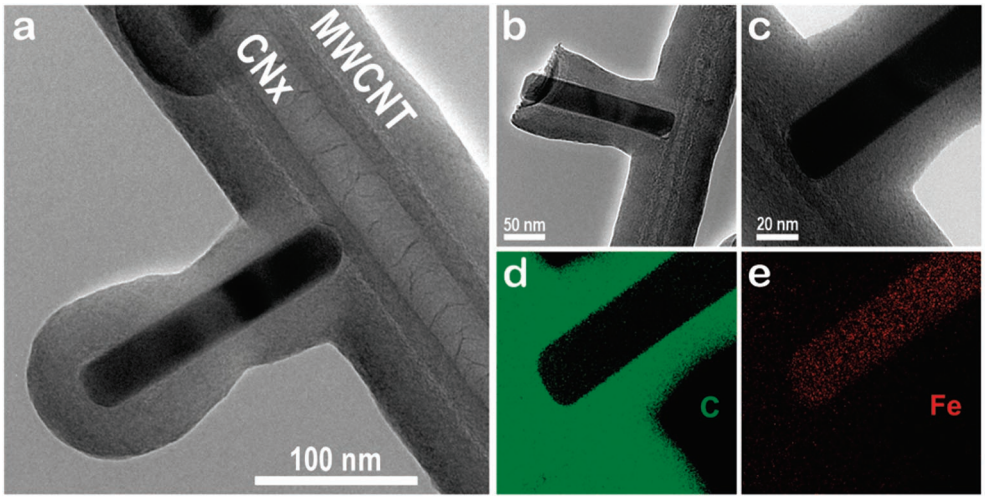

Figure 4. TEM and EELS mappings on the heteronanotubes. (a) HRTEM image exhibiting a MWCNT attached in a "T" junction on a CN_x nanotube. (b) A similar structure in detail and a close-up of the interface between the metal and the surface of the MWNT-CN_x. (c) Higher magnification of another representative heteronanotube showing the Fe rod. (d) Carbon and (e) Fe EELS mappings of image shown in (c).

these rods consist of elemental Fe only (see Figures 4d,e); we never observed oxygen in these systems.

X-ray powder diffraction patterns (not shown here) illustrate differences between the original product (pristine CN_x nanotubes) and the final product (CN_x@CNT junctions). For example, the heterojunction material obtained from the Fe clusters deposited from $K_3[Fe(CN)_6]$ revealed the signal of cohenite (orthorhombic Fe_3C). Since additional Fe was deposited on the tubes after the chemical coating process, we also noted an increase in the intensity of the Fe (bcc phase) reflections after the second CVD process. More interestingly, TGA analysis of CN_x@CNT material in air (see Figure 5) displayed two separate decomposition temperatures, one 86 °C below and the other 69 °C above the characteristic decomposition temperature of pristine MWNTs-CN_x (T_{dec} = 378 °C). The presence of two decomposition temperatures upon oxidation confirms the existence of two different types of tubular structures. Note that these decomposition temperatures are lower than those observed for highly crystalline MWCNTs (T_{dec} = 476 °C).

To determine which coaxial structures decomposes first, we heated the sample in air just above the first decomposition temperature recorded at ca. 300 °C, and subsequently we analyzed the remains by scanning transmission electron microscopy (STEM). The remaining nanotubes exhibited the characteristic morphology of MWNTs-CN_x (see inset in Figure 5), which confirmed that the structure that decomposes first is the low-crystalline outer (pure C) MWNTs shells. The reason for the oxidation resistance observed by the second peak 70 °C above the first one could be rationalized as a consequence of the annealing process at which these nanotubes were submitted during first stage of the second CVD treatment. This thermal annealing therefore enhanced the crystallinity of the MWNTs-CN_x. Therefore, these TGA studies suggest that the heteronanotubes are more chemically active than highly crystalline MWNTs.

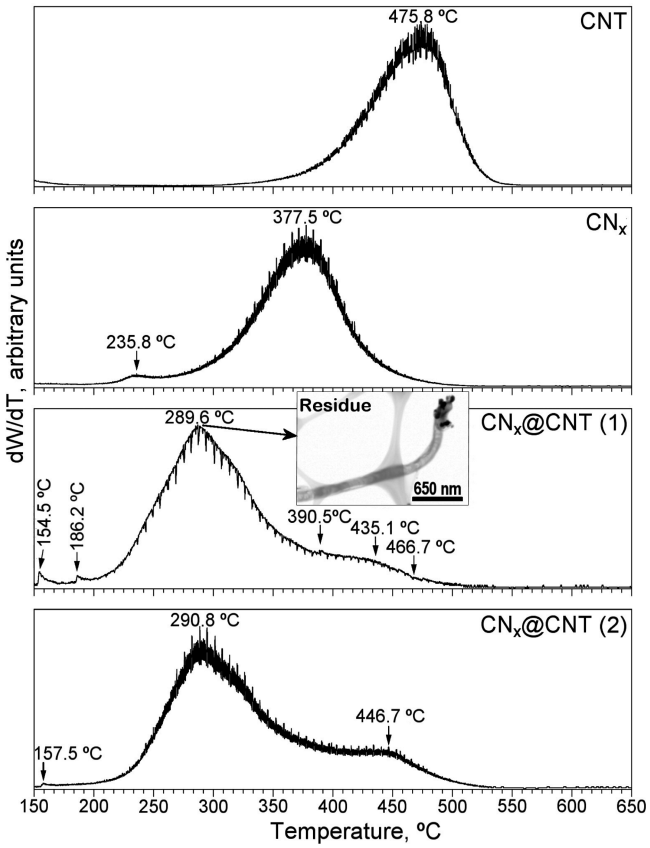

Figure 5. First derivative of TGA analysis of heteronanocables and control samples. From top to bottom: Thermal decomposition curve for MWCNTs and MWNTs-CN_x, followed by the curves corresponding to two of the coaxial CN_x@CNT samples. Inset: STEM image of the residue remaining after heating in air up to the first decomposition temperature (ca. 290 °C).

On the basis of the results discussed above, we propose a possible growth mechanism for producing nanotube coaxial junctions, as depicted in Figure 6. As previously stated, the MWNTs-CN_x seemed to react with $K_3[Fe(CN)_6]$ in an acidic

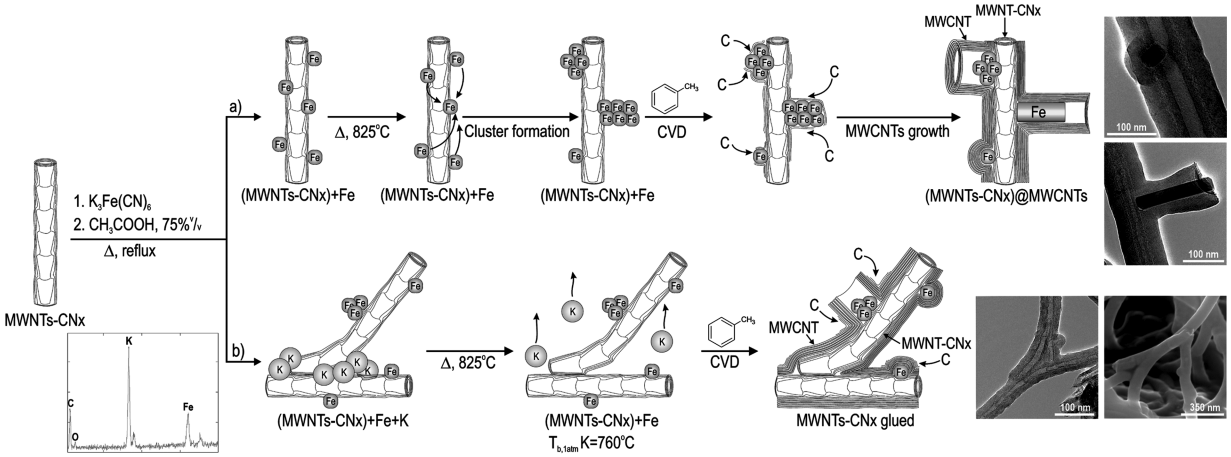

Figure 6. Schematic of the growth mechanism proposed for branched coaxial carbon nanotubes. The starting material (left) is MWNT-CN_x reacted with $K_3[Fe(CN)_6]$, containing potassium and an amount of Fe higher than that found in the pristine CN_x nanotubes, as shown in an EDX spectrum. (a) Growth of nanotube branches and coaxial structures: Iron nanoparticles migrate and coalesce into bigger clusters during heating to 825 °C. At that temperature, toluene is introduced and the iron clusters catalyze the formation of MWCNT branches; additionally, graphene sheets form a continuous wrapping around the MWNT-CN_x. (b) Growth of "on-junctions" and coaxial nanocables: The potassium present in the samples could act as binder before it evaporates to keep the tubes and bundles together before the additional carbon is deposited on the surface. Simultaneously, Fe cluster formation occurs which catalyzes the growth of additional pure MWCNT.

medium, which is known to protonate CN_x tubes, as revealed by their good dispersion in acidic aqueous solutions, whereas MWCNTs were not (see Supporting Information). MWCNTs, on the other hand, when subjected to the same treatment, are seen to be irregularly coated by large crystals (results not shown here). Therefore, we suggest that the N sites of the CN_x tubes are protonated and facilitate the coating by anionic metal complexes.

An EDX spectrum (shown in Figure 6, bottom left) of the Fe coated CN_x tubes reveals the presence of potassium and higher amounts of Fe (19 wt %) when compared to the as-produced MWNTs-CN_x (6.75 wt %). During annealing in Ar, prior to the introduction of the pristine toluene aerosol into the reactor, the coordination sphere of $K_3[Fe(CN)_6]$ breaks (this process would occur below 400 °C) and produces gaseous hydrogen cyanide (HCN), thus leaving behind metal atoms that are able to aggregate into clusters. Subsequently, these Fe nanoparticles could migrate and coalesce into larger agglomerates (e.g., rods seen in Figure 4). These Fe agglomerates then act as catalytic sites for growing new MWNTs when the toluene decomposes on the Fe−CN_x system at 825 °C. At this point, potassium is expected to be evaporated (its boiling point is 760 °C at 1 atm). However, potassium could act as a binder agent before its evaporation, keeping the CN_x together for the formation of on-junctions (as in Figure 6) and other types. It is important to stress that the formation of new carbon nanotubes growing normally from the MWNTs-CN_x and the concentric layers deposited on the doped tubes appear to occur simultaneously. This implies that the iron clusters located on the tubes (acting as a substrate) could promote the formation of carbon layers capable of being deposited homogenously over the whole CN_x tubes surface. The deposition of such graphitic coatings could continue until two growing fronts meet and coalesce into a continuous cylindrical structure, thus forming on-type junctions (Figure 1i). Similarly, if the merge of a normally growing MWNT over a cylindrically growing MWNT coating occurs, other fused networks result.

The repeated occurrence of this process results in the formation of the branched 3D nanotube structures exhibiting an outer coaxial cover of pure C on the CN_x tubes. We also note that when iron particles are deposited on a substrate, they usually catalyze the formation of nanotubes, growing only perpendicularly to the substrate, without fusing into other growing tubes to form networks.

The method reported in this letter enabled us to produce novel structures not achievable by previously reported techniques used to create CNTs−covalent junction structures.[30−39] Such methods are not only very different from ours, but they are clearly unable to produce the kinds of *coaxial heterostructures* we observed in this study.

In summary, a two-step technique was successfully used to produce new families of CN_x@CNTs nanotube junctions. The initial step consists of using one of the two different methods for depositing Fe clusters on N-doped carbon nanotubes taking advantage of the chemical properties inherent to CN_x, and the second consisted of a thermal treatment in the presence of a toluene aerosol. We believe that this technique could be important in creating various nanostructured carbon materials such as junctions and ordered nanoscale arrangements of nanotubes. Different types of heterojunctions were identified (e.g. "Y", "T", multi-branched, and "on-junctions"). The detailed characterization of these materials enabled us to propose a possible growth mechanism. This is, to the best of our knowledge, the first report on the production of coaxial nanocables composed of an internal core of one or more doped nanotubes, MWNTs-CN_x, and an external concentric shell of pure carbon MWNTs. We note that the method we proposed here is one of the first approaches to actually exploit the chemistry of the N-doped carbon nanotubes to create new nanostructured materials. We expect to witness more specific reactions

considering the N site as chemically active in other research reports. We also emphasize that these coaxial heterostructures had not even been proposed theoretically, and this account demonstrates an easy way to synthesize them, thus opening up new avenues to study the controlled growth of coaxial nanotubes and junctions. In addition, we believe that the electrical and mechanical properties of these networks may be fascinating, but they are outside the scope of this paper. Therefore, further and detailed characterization on individual heterojunctions is needed.

As reported in the literature,[23,24,40,41] the electrical conductivity of carbon nanotubes could increase depending on the N content within the tubules, being able to behave as a metal due to the injection of electronic states in the graphene sheet by the nitrogen atoms. In the same way, standard (pure carbon) MWNTs could behave as semiconductors, and if they exhibit lower crystallinity, the electrical conductivity could be reduced significantly. Following this rationalization, the CN_x tubes' cores could exhibit higher electrical conductivity when compared to the outer shell (undoped and more defective), relevant in the fabrication of novel nanoelectronic devices.

We believe that these heteronetworks could also be used as templates for embedding polymers in the production of novel shock absorber composites. In addition, these networks could serve as catalytic supports, damping devices, and filters. Such suggestions only take advantage of the physical structure of the random network, but it should be clear that the nanotube networks reported here may also find multiple applications beyond those suggested in this study. Some potentially exciting applications, in electronics and optics for example, would require the controlled production of coaxial junctions and well-defined networks to create circuits or waveguide devices. Therefore, further experimental and theoretical research should be carried out in order to better understand their properties and control their production.

Acknowledgment. We thank CONACYT-Mexico for graduate school fellowship (X.L.) and grants: SEP-2004-45772, C02-41464-Inter American Materials Collaboration, SALUD-2004-C01-013, PUE-2004-CO2-9 Fondos Mixtos CONACYT-Puebla (M.T.), SEP-2004-47338 (Y.I.V.C.), and SEP-2004-47337 (F.J.R.M.). We also thank Humberto Terrones for partial support from grant C02-42428-Inter American Materials Collaboration and IPICYT for additional financial support for finishing this manuscript (X.L.).

Supporting Information Available: Solubility test of MWNTs-CN_x vs MWCNTs in a protic medium. This material is available free of charge via the Internet at http://pubs.acs.org.

References

(1) Oberlin, A.; Endo, M.; Koyama, T. *J. Cryst. Growth* **1976**, *32*, 335−349.
(2) Ijima, S. *Nature* **1991**, *354*, 56−58.
(3) Iijima, S.; Ichihashi, T. *Nature* **1993**, *363*, 603−605.
(4) Bethune, D. S.; Klang, C. H.; de Vries, M. S.; Gorman, G.; Savoy, R.; Vazquez, J.; Beyers, R. *Nature* **1993**, *363*, 605−607.
(5) Teo, K. B. K.; Singh, C.; Chhowalla, M.; Milne, W. I. Catalytic Synthesis of Carbon Nanotubes and Nanofibers. In *Encyclopedia of Nanoscience and Nanotechnology*; Nalwa, H. S., Ed.; American Scientific Publishing: New York, 2003; Vol. 10, pp 1−22.
(6) Baughman, R. H.; Zakhidov, A. A.; de Heer, W. A. *Science* **2002**, *297*, 787−792.
(7) Terrones, M. *Annu. Rev. Mater. Res.* **2003**, *33*, 419−501.
(8) Troiani, H. E.; Miki-Yoshida, M.; Camacho-Bragado; Marques, M. A. L.; Rubio, A.; Ascencio, J. A.; Jose-Yacaman, M. *Nano Lett.* **2003**, *3*, 751−755.
(9) Rueckes, T.; Kim, K.; Joselevich, E.; Tseng, G. Y.; Cheung, C.-L.; Lieber, C. M. *Science* **2000**, *289*, 94−97.
(10) Derycke, V.; Martel, R.; Appenzeller, J.; Avouris, P. *Nano Lett.* **2001**, *1*, 453−456.
(11) Bachtold, A.; Hadley, P.; Nakanishi, T.; Dekker, C. *Science* **2001**, *294*, 1317−1320.
(12) Collins, P. G.; Arnold, M. S.; Avouris, P. *Science* **2001**, *292*, 706−709.
(13) Planeix, J. M.; Coustel, N.; Coq, B.; Brotons, V.; Kumbhar, P. S.; Dutartre, R.; Geneste, P.; Bernier, P.; Ajayan, P. M. *J. Am. Chem. Soc.* **1994**, *116*, 7935−7936.
(14) Joo, S. H.; Choi, S. J.; Oh, I.; Kwak, J.; Liu, Z.; Terasaki, O.; Ryoo, R. *Nature* **2001**, *412*, 169−172.
(15) Rodriguez, N. M.; Chambers, A.; Baker, T. K. *Langmuir* **1995**, *11*, 3862−3866.
(16) Ouyang, M.; Huang, J.-L.; Cheung, C. L.; Lieber, C. M. *Science* **2001**, *291*, 97−100.
(17) Park, J.; Daraio, C.; Jin, S.; Bandaru, P. R.; Gaillard, J.; Rao, A. M. *Appl. Phys. Lett.* **2006**, *88*, 243113.
(18) Sun, X.; Li, R.; Stansfield, B.; Dodelet, J. P.; Désilets, S. *Chem. Phys. Lett.* **2004**, *394*, 266−270.
(19) Ting, J.-M.; Li, T.-P.; Chang, C.-C. *Carbon* **2004**, *42*, 2997−3002.
(20) Collins, P. G.; Zettl, A.; Bando, H.; Thess, A.; Smalley, R. E. *Science* **1997**, *278*, 100−103.
(21) Terrones, M.; Banhart, F.; Grobert, N.; Charlier, J. C.; Terrones, H.; Ajayan, P. M. *Phys. Rev. Lett.* **2002**, *89*, 075505.
(22) Banhart, F. *Nano Lett.* **2001**, *1*, 329−332.
(23) Xie, R.-H.; Zhao, J.; Rao, Q. Doped Carbon Nanotubes. In *Encyclopedia of Nanoscience and Nanotechnology*, Nalwa, H. S., Ed.; American Scientific Publishers: New York, 2004; Vol. 10, pp 1−31.
(24) Czerw, R.; Terrones, M.; Charlier, J. C.; Blase, X.; Foley, B.; Kamalakaran, R.; Grobert, N.; Terrones, H.; Ajayan, P. M.; Blau, W.; Tekleab, D.; Rühle, M.; Carroll, D. L. *Nano Lett.* **2001**, *1*, 457−460.
(25) Jiang, L.; Gao, L. *Carbon* **2003**, *41*, 2923−2929.
(26) Jia, N.; Wang, L.; Liu, L.; Zhou, Q.; Jiang, Z. *Electrochem. Commun.* **2005**, *7*, 349−354.
(27) Kamalakaran, R.; Terrones, M.; Seeger, T.; Kohler-Redlich, P.; Rühle, M.; Kim, Y. A.; Hayashi, T.; Endo, M. *Appl. Phys. Lett.* **2000**, *77*, 3385−3387.
(28) Mayne, M.; Grobert, N.; Terrones, M.; Kamalakaran, R.; Rühle, M.; Kroto, H. W.; Walton, D. R. M. *Chem. Phys. Lett.* **2001**, *338*, 101−107.
(29) Pinault, M.; Mayne-L'Hermite, M.; Reynaud, C.; Pichot, V.; Launois, P.; Ballutaud, D. *Carbon* **2005**, *43*, 2968−2976.
(30) AuBuchon, J. F.; Chen, L.-H.; Daraio, C.; Jin, S. *Nano Lett.* **2006**, *6*, 324−328.
(31) Satishkumar, B. C.; Thomas, J. P.; Govindaraj, A.; Rao, N. R. *Appl. Phys. Lett.* **2000**, *77*, 2530−2532.
(32) Gan, B.; Ahn, J.; Zhang, Q.; Rusli; Yoon, S. F.; Huang, Q.-F.; Chew, K.; Ligatchev, V. A.; Zhang, X.-B.; Li, W.-Z. *Chem. Phys. Lett.* **2001**, *333*, 23−28.
(33) Gothard, N.; Daraio, C.; Gaillard, J.; Zidan, R.; Jin, S.; Rao, A. M. *Nano Lett.* **2004**, *4*, 213−217.
(34) Gu, P.; Zhao, J. H.; Li, G. H. *J. Mater. Res.* **2002**, *17*, 2768−2770.
(35) Li, J.; Papadopoulos, C.; Xu, J. *Nature* **1999**, *402*, 253−254.
(36) Meng, G.; Jung, Y. J.; Cao, A.; Vajtai, R.; Ajayan, P. M. *Proc. Natl. Acad. Sci. U.S.A.* **2005**, *102*, 7074−7078.
(37) Ma, X.; Wang, E. G. *Appl. Phys. Lett.* **2001**, *285*, 978−980.
(38) Chai, Y.; Zhang, Q. F.; Wu, J. L. *Carbon* **2006**, *44*, 687−691.
(39) Wei, D.; Liu, Y.; Cao, L.; Fu, L.; Li, X.; Wang, Y.; Yu, G.; Zhu, D. *Nano Lett.* **2006**, *6*, 186−192.
(40) Terrones, M.; Ajayan, P. M.; Banhart, F.; Blase, X.; Carroll, D. L.; Charlier, J. C.; Czerw, R.; Foley, B.; Grobert, N. *Appl. Phys. A* **2001**, *74*, 355−361.
(41) Lim, S. H.; Elim, H. I.; Gao, X. Y.; Wee, A. T. S.; Ji, W.; Lee, J. Y.; Lin, J. *Phys. Rev. B* **2006**, *73*, 045402.

NL0706502